Pressure-dependent flow behavior of $Zr_{41.2}Ti_{13.8}Cu_{12.5}Ni_{10}Be_{22.5}$ bulk metallic glass

Jun Lu and Guruswami Ravichandran[a)]
Graduate Aeronautical Laboratories, California Institute of Technology, Pasadena, California 91125

(Received 19 November 2002; accepted 7 May 2003)

An experimental study of the inelastic deformation of bulk metallic glass $Zr_{41.2}Ti_{13.8}Cu_{12.5}Ni_{10}Be_{22.5}$ under multiaxial compression using a confining sleeve technique is presented. In contrast to the catastrophic shear failure (brittle) in uniaxial compression, the metallic glass exhibited large inelastic deformation of more than 10% under confinement, demonstrating the nature of ductile deformation under constrained conditions in spite of the long-range disordered characteristic of the material. It was found that the metallic glass followed a pressure (p) dependent Tresca criterion $\tau = \tau_0 + \beta p$, and the coefficient of the pressure dependence β was 0.17. Multiple parallel shear bands oriented at 45° to the loading direction were observed on the surfaces of the deformed specimens and were responsible for the overall inelastic deformation.

I. INTRODUCTION

Since the discovery of the first metallic glass in the form of a thin ribbon by Klement *et al.*,[1] many metallic glasses in binary and ternary alloy systems were developed prior to the 1980s.[2–4] However, high critical quenching rate (10^3–10^7 K/s) required to form these metastable materials imposed a limit on the attainable sizes (typically smaller than a millimeter) for these metallic glass samples, mainly due to factors such as thermal stability and conductivity of these materials during the undercooling process. The scatter in geometric properties made accurate measurement of mechanical properties extremely difficult and less reliable. The application of metallic glasses as structural materials was impossible until the recent development of bulk metallic glasses of centimeter-scale thickness using relatively inexpensive materials and simple processing techniques in the last decade.[5,6]

One of the most important bulk metallic glass families, named Vitreloy family, has been recognized as an intriguing class of potential structural amorphous material (SAM). One of the most thoroughly studied bulk metallic glasses is Vitreloy 1,[7] i.e., $Zr_{41.2}Ti_{13.8}Cu_{12.5}Ni_{10}Be_{22.5}$ (commonly referred to as Vit 1), which has many desirable properties such as high specific strength and hardness, corrosion resistance, and near-net-shape casting ability.[6,8–10] It is being applied as a structural material in coatings, electronic packaging, sporting equipment, and defense purposes.[10]

At elevated temperatures near or above its glass-transition temperature, Vitreloy 1 exhibits nonlinear viscoelastic behavior, and its deformation behavior can be well characterized.[11] However, at low temperature (e.g., room temperature), the high strength metallic glass deforms elastically and fails in a brittle and catastrophic manner, although one may expect the material to be ductile because of its metallic bonding. While the study of high-temperature homogeneous deformation behavior[11] can assist in understanding the net-shape thermal casting process of Vitreloy 1, the deformation behavior of Vit 1 at low temperatures (lower than its glass-transition temperature) is directly related to the structural applications of the material. Only limited inelastic strains (<1%) can be achieved at room temperature in Vitreloy 1 under uniaxial loading condition.[11,12] Room-temperature ductility is impaired by catastrophic shear failure caused by shear localization, which is the primary and dominant inelastic deformation mechanism for metallic glasses. The shear band formation in metallic glasses can be regarded as a "material instability" or "nucleation" of material imperfection. Therefore, it is not trivial to establish inelastic constitutive laws and to validate hypotheses in the literature that are often conflicting: to examine if the flow stress of a metallic glass under multiaxial stress state is a function of hydrostatic pressure and/or normal stress.

Experiments on metallic glasses have suggested that their yield stress could be either normal stress dependent, pressure dependent, or follow the pressure-independent von Mises flow criterion.[12–20] Bruck *et al.* performed uniaxial tension and compression experiments, as well as pure torsion experiments on Vit 1, and concluded

a)Address all correspondence to this author.
e-mail: ravi@caltech.edu

that the yield stress for the material is pressure independent and would obey the von Mises flow criterion.[12] They were further reassured of their conclusion by the observation that the shear failure in specimens occurred at an angle of 45° to the loading axis under uniaxial tension and compression. Vaidyanathan *et al.*[16] used microindentation to study the flow behavior of Vit 1 and concluded that the yield stress of the material follows the Mohr–Coulomb criterion. Lewandowski and coworkers[17–19] investigated the flow criterion for Vit 1 subjected to a uniform axial tensile or compressive stress with lateral compressive stress. This investigation suggested that Vit 1 has a negligible pressure-dependent behavior and that the yield stress of Vit 1 may be characterized by a normal stress-dependent flow criterion.

Indentation provides a means of constraining shear band propagation by surrounding elastic material that is not severely deformed. In addition, high pressures are present in the region directly underneath indentation contact zone. Uniaxial deformation[11] and dynamic indentation experiments[20] indicate that the yield stress of Vit 1 is strain rate independent at temperatures lower than the glass-transition temperature (623 K). Indeed, the deformation of Vit 1 may be approximated by the von Mises flow criterion under uniaxial loading conditions. However, the indentation studies[16,20] indicate that the yield stress of Vit 1 is dependent on either the normal stress or the pressure under both static and dynamic loading conditions. However, the indentation studies are not capable of discerning whether a pressure or normal stress dependent (e.g., Mohr-Coulomb) model is more suitable for metallic glasses (in particular for Vit 1) or not.

Another possible way of arresting shear bands during deformation of metallic glasses is to use confining sleeves or high-pressure vessels. Complimentary to the experimental technique used in the experiments by Lewandowski and coworkers,[17–19] a simple experimental technique was used in the present study to further investigate the effect of stress state on the flow behavior of metallic glasses under multiaxial loading conditions. Specific attention is focused on the inelastic deformation of Vitreloy 1 under "simple" multiaxial compression by sleeve-confinement technique at quasistatic strain rates. The term "multiaxial stress state" used here refers to the axial compression of a cylindrical specimen with nominally proportional lateral compressive confinement. This stress state corresponds to a compressive stress state in all three principal directions, and the confining stress that can be applied is as high as 2 GPa (resulting in a hydrostatic pressure as high as 2.5 GPa), which is substantially higher than that achieved in previous studies.[17–19] The experimental technique for imposing multiaxial compression is described in Sec. II. Under such a stress state, the resulting inelastic deformation is characterized, and the resulting shear band patterns are examined in Sec. III. A pressure-dependent flow criterion is formulated based on the experimental results in Sec. IV. The strain rate independence of Vit 1 at room temperature[11] implies that the study of the quasistatic flow behavior of Vit 1 under lateral confinement could be used to interpret the behavior of Vit 1 in the dynamic loading regime as well. The conclusions for the present study are summarized in Sec. V.

II. EXPERIMENTAL

A. Material

The material used in this study is $Zr_{41.2}Ti_{13.8}Cu_{12.5}Ni_{10}Be_{22.5}$ (commercially known as Vitreloy 1 or Vit 1), which is one of the best metallic glass formers ever developed.[7] It has excellent thermal stability against crystal nucleation, resulting quite easily in a glassy sample on the centimeter scale, and making possible an experiment that uses a confining sleeve. Ingots of alloys were made by a mixture of the metallic elements in a silver/copper boat or an arc-melter on a water-cooled copper plate, under a titanium gettered argon atmosphere (copper with purity of 99.999%, nickel with purity of 99.995%, and titanium with purity of 99.995% were supplied by Cerac, Inc., Milwaukee, WI. Zirconium with purity of 99.5% was supplied by Teledyne Wah-Chang, Inc., Albany, OR, and beryllium with purity of 99.99% was supplied by Electronic Space Products International, Ashland, OR). To maintain the homogeneity of the ingot, copper, nickel, and titanium were molten together in one batch and then the zirconium and beryllium were molten in a second batch. Finally, they were remelted together for a few minutes until a homogeneous sample was formed. Subsequently, the liquid was undercooled by stopping the heating to form a glassy ingot.

As a last step of achieving a homogenous sample, the ingot was cut into smaller pieces, which were then remelted at a temperature of 1200 K, which is higher than the liquidus temperature (993 K) of Vitreloy 1 and much lower than the melting temperature of quartz. This was done in a sealed quartz tube of 10 mm in diameter under high vacuum condition ($<10^{-6}$ torr) followed by slow quenching in water at a cooling rate higher than 1 K/s. Precautions were taken to process the material with as low an oxygen content as possible since it has been shown that high oxygen content can adversely affect the processing and the microstructure.[17–19] The quenched rod of 8–10 mm long was ground to remove the attached quartz contaminant and a few millimeters of outer layer. The amorphous state of the ground Vit 1 thus processed was verified by x-ray diffraction. The processing and physical properties of this material are well documented in the literature.[7,12,21,22] The physical and mechanical properties of Vit 1 made using the approaches described above are listed in Table I.

B. Specimen

The casting rods made using the quartz casting method were then centerless ground to the desired diameters of 3.81 mm (i.e., 0.15 in., used for "A" size specimen), 5.08 mm (i.e., 0.20 in., used for "B" size specimen), and 6.35 mm (i.e., 0.25 in., used for "C" size specimen) with a surface finish of 6 μm. Subsequently, the rods were cut using a low speed precision diamond saw into compression specimens with 1:1 to 1.5:1 length-to-diameter ratio. A larger aspect ratio was not considered in the present study to reduce the effect of friction between the sleeves and the specimens. Subsequently, the end faces of each specimen, clamped with a specially designed mounting block, were polished down to 6-μm surface finish. The main purpose of the mounting block was to keep the polished surface flat while ensuring the two end surfaces of each specimen were made parallel to each other within a tolerance of 10-μm gap. A total of 14 specimens were fabricated following the procedures described above. The size of the specimens and other relevant experimental conditions are summarized in Table II.

C. Compression fixture

A servo-hydraulic material testing system (MTS; with a 319 series axial/torsional load frame and 358 series load units) (MTS Systems Corporation, Eden Praire, MN) was used to apply axial compression on the confined specimens. The compression fixture used in the experiments is illustrated in Fig. 1. Confined specimens are sandwiched in between two finely polished tungsten carbide inserts of the same cross section as that of the specimens. The load acting on the inserts is transferred through two larger polished tungsten carbide disks onto the loading rods made of heat-treated [482 °C (900 °F) for 6 h] C300 maraging steel (compressive yield strength, 2.26 GPa), which are aligned with two precision linear ball bearings installed in a solid 2024 aluminum frame. High-pressure lubricant (extreme-pressure Moly-Graph multipurpose grease, STA-Lube, Inc., Rango Dominquez, CA) was applied onto the contacting surfaces of the specimens, sleeves, and inserts to reduce friction among them.

TABLE I. Mechanical properties of Vitreloy 1 and C300 maraging steel.

Property	Vitreloy 1	C300 maraging steel
Density (g/cm^3)	6.0	8.0
Young's modulus (GPa)	96[a]	200[a]
Poisson's ratio	0.36[a]	0.3[a]
Elastic strain limit	0.02[12]	0.011[b]
Yield strength (GPa)	1.90[12]	2.26[b]
Vickers hardness (kg/mm^2)	540[8]	…

[a]Deduced from ultrasonic measurements.
[b]Determined from compression experiment.

TABLE II. Specimen dimensions and experimental conditions.

Experiment	l (mm)[a]	a (mm)[b]	b (mm)[c]	b/a	σ_c^{max} (MPa)[d]	p^{max} (MPa)[e]	ϵ_0[f]
C1	6.09	6.11	7.62	1.25	501	1150	~0.06
A2	5.86	3.81	5.33	1.4	761	1450	~0.09
A1	3.68	3.81	7.62	2.0	1570	2420	~0.10
B3	5.01	5.08	10.16	2.0	1448	2230	~0.03
C4	6.67	6.34	25.40	4.0	1697	2500	~0.03
B4	4.97	5.08	25.40	5.0	1883	2790	~0.06

[a]l = length of the specimen.
[b]a = diameter of the specimen.
[c]b = outer diameter of the confining sleeve.
[d]σ_c^{max} = maximum confining stress.
[e]p^{max} = maximum hydrostatic pressure.
[f]ϵ_0 = maximum inelastic strain.

D. Radial confinement

The lateral confinement to the material was realized by inserting the cylindrical specimen into the cavity of a hollow cylinder. The confining cylinder provides restraint against radial expansion, thus generating a uniform lateral stress on the specimen surface along the radial direction perpendicular to the loading axis. Ideally, it is assumed that the inner diameter of the sleeve is exactly the same as that of the specimen. The effect of the mismatch of these two diameters on the measurement of confining stress will be examined later in this section. It is also assumed that the deformation of the confining sleeve remains uniform during compression so that a strain gage placed on the outer surface of the sleeve along the hoop direction represents the uniform hoop strain everywhere on the outer surface of the sleeve. In addition, it is assumed that the friction in between the specimen and the sleeve is negligible so that a simple

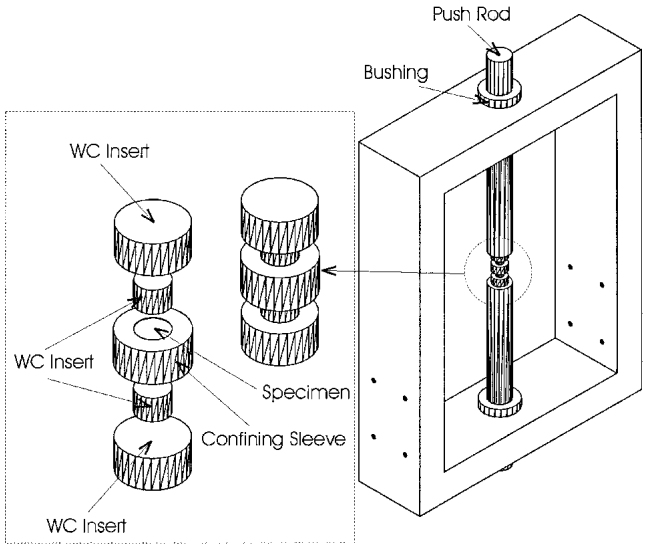

FIG. 1. Quasistatic compression fixture and the radial confinement apparatus.

analytical solution can be applied in deducing relevant quantities such as the confining stress. It is necessary to mention that the confining stress refers to the radial stress (or normal stress) exerted on the cylindrical specimen, and not the hydrostatic pressure in the specimen. Assuming that both the sleeve and the specimen deform elastically, one can estimate the radial confining stress,

$$\sigma_c = \frac{\sigma \nu / E}{\left(\frac{b^2 + a^2}{b^2 - a^2} + \nu_s\right)/E_s + (1 - \nu)/E} \quad , \qquad (1)$$

where E and E_s are the Young's modulus of the sleeve and the specimen materials, respectively; ν and ν_s are the Poisson's ratio of the specimen and the sleeve materials, respectively; a is the diameter of the specimen and the inner diameter of the sleeve; b is the outer diameter of the sleeve; and σ is the loading stress in the axial direction. Assuming that the sleeve deforms elastically, after the specimen material yields, the confining stress becomes

$$\sigma_c = \frac{E_s}{2}\left(\frac{b^2}{a^2} - 1\right)\epsilon_\theta^{out} \quad , \qquad (2)$$

where ϵ_θ^{out} is the hoop strain at the outer surface of the sleeve. The state of stress in the specimen can be thus determined based on the hoop strain as well as the axial deformation and stress.

Oguni *et al.*[23] utilized this method of using elastically deforming sleeves made of aluminum to apply radial confinement in studying the multiaxial deformation and failure behavior of unidirectional E-glass/vinylester composites. Ma *et al.*[24] used 4340 steel sleeves to study multiaxial deformation behavior of a polymer, namely, polycarbonate. The materials used in these studies had relatively low strength, in which case the sleeves experienced only elastic deformation during the entire compression process. However, metallic glasses have high yield strength; for example, Vit 1 has yield strength of about 1.9 GPa under uniaxial compression. Therefore, the assumption of the confining sleeve remaining elastic during deformation may not be realistic. Calculations have shown that only high strength materials like tungsten carbide (failure strength ~ 4 GPa) may possibly meet the requirement of having only elastic deformation in the confinement sleeve. However, besides the high cost of obtaining and grinding such a material, its high Young's modulus indicates that tungsten carbide is a very stiff material and is not quite suitable to allow radial inelastic expansion of the specimen resulting in high frictional stress.

Of the available high strength materials, maraging C300 steel is selected since it has high yield stress (2.26 GPa), relatively large strain (~8%) to failure, and moderate value of Young's modulus (210 GPa). Compression experiments were performed on heat-treated C300 samples (Table I), and it was found that C300 has a negligible strain hardening effect such that an elastic-rigid plastic model can be used to approximate its constitutive behavior. Before the sleeve yields, Eqs. (1) and (2) are valid for computing the confining stress. After the sleeve begins to yield, the boundary between the elastic and plastically deformed zones in the sleeve, i.e., the radial location ρ where the sleeve starts to yield (elastic-plastic boundary), can be expressed as

$$\rho = b\sqrt{\frac{\epsilon_\theta^{out} E_s}{\sigma_s}} \quad , \qquad (3)$$

where σ_s is the yield stress of the sleeve material. When this situation is reached, the corresponding confining stress σ_c becomes

$$\sigma_c = \sigma_s\left[\ln\frac{\rho}{a} + \frac{1}{2}\left(1 - \frac{\rho^2}{b^2}\right)\right] \quad . \qquad (4)$$

The maximum confining pressure that can be achieved according to Eq. (4) is

$$\sigma_c^{max} = \sigma_s \ln\frac{b}{a} \quad . \qquad (5)$$

If the sleeve yields, Eqs. (3) and (4) and the axial stress in the loading direction fully describe the stress state in the material.

The hoop strain on the outer surface of the confining sleeve was measured using a strain gauge [Micro-Measurements, Raleigh, NC CEA-06-062UW (or AQ-350)] mounted on the outer surface. The strain gage was connected to a Wheatstone bridge with a 10 V direct current (dc) power supply. All the signals including the load and displacement from the servo hydraulic MTS were recorded using a 4-channel Nicolet 440 digital oscilloscope (Nicolet Instrument Technologies, Madison, WI). The inner diameter of the confining sleeve was carefully ground or honed to provide minimum size misfit in between the sleeve and the specimen. The error caused by a size mismatch between the specimen and the sleeve will be discussed in Sec. III. The outer diameter (Table II) of the confining sleeve was chosen such that the diameter ratio (b/a) of 1.4, 2.0, 4.0, and 5.0 was realized to achieve various confining stress levels. For realistic dimensions of the specimen and the sleeve, the maximum possible confining stress that can be achieved is calculated to be around 400 to 1000 MPa if the sleeve deforms only elastically. Actually, for a specimen made of Vit 1 metallic glass, both the specimen and the sleeve will yield, leading to larger confining stress as can be seen in the experiments described in the next section. On the other hand, the maximum confinement stress is also limited by the strength of the tungsten carbide inserts whose nominal failure stress is around 4 GPa.

III. RESULTS

Multiaxial compression experiments under lateral confining stress imposed by the sleeves were performed at a nominal axial quasi-static strain rate of 10^{-3} s^{-1} using the servo hydraulic MTS. The evolution of the hoop strain on the outer surface of sleeve, axial stress and axial displacement of the cylindrical Vit 1 specimen were recorded. The ratio between the outer diameter (b) and the inner diameter (a) of the sleeve was varied in the range of 1.25–5.0, which provided confining stress of up to 2000 MPa. Further increase in the ratio b/a was not considered because it induces relatively little increase in the confining stress beyond the value mentioned above.

The hoop strain was obtained directly from the strain gauge signal, and the axial stress and strain were calculated using the axial load and displacement as well as the compliance of the MTS loading frame. The relationship between the confining stress and the hoop strain needs to be determined in each experiment for establishing the loading path experienced by the specimen. To do this, it is necessary to establish the confining stress σ_c^{elas}, where the inner surface of the confining sleeve begins to yield. By resorting to Eqs. (2) and (4), the hoop strain ϵ_0 associated with σ_c^{elas} can be numerically solved using the following equation:

$$\frac{E_s}{2}\left(\frac{b^2}{a^2}-1\right)\epsilon_0 = \sigma_s\left[\ln\left(\frac{b}{a}\sqrt{\frac{\epsilon_0 E_s}{\sigma_s}}\right)+\frac{1}{2}\left(1-\frac{\epsilon_0 E_s}{\sigma_s}\right)\right] . \quad (6)$$

If $\epsilon_\theta^{out} \le \epsilon_0$, the confining sleeve is in the elastic range and Eq. (2) is used to calculate the confining stress. If $\epsilon_\theta^{out} > \epsilon_0$ and $\rho < b$, part of the confining sleeve yields and Eq. (4) is used to calculate the confining stress. But if ϵ_θ^{out} increases further, such that $\rho = b$, and the confining sleeve completely yields, the confining stress is the same as that when $\rho = b$ is initially reached.

A. Stress–strain response

A typical stress–strain curve for Vit 1 under uniaxial compression condition is linear up to a strain of about 0.02 (Young's modulus $E = 95$ GPa) followed by yielding due to shear band nucleation and propagation. Catastrophic shear failure occurs immediately following yield and a very limited amount of macroscopic inelastic strain that never exceeds 0.01. The maximum uniaxial compressive stress is in the range of 1.90–1.93 GPa.[11,12]

The relevant experimental conditions and associated parameters for the confinement experiments are listed in Table II. Figure 2 shows the mechanical response of Vit 1 using a confinement sleeve with the ratio, $b/a = 1.25$. The sleeve remained initially in the elastic range and the confining stress was proportional to the hoop strain before the hoop strain reaches a value of 0.0069. As the hoop strain increased further ρ the radius of the elastic-plastic boundary inside the sleeve increased correspondingly until the sleeve completely yielded, indicating the maximum confining stress was reached. The yielding occurred after the confining stress reached 404 MPa, and after the sleeve was completely yielded, the increase in the axial stress was negligible. The measured hoop strain reached a value of 0.016 before the sleeve was broken. The axial stress–strain curve and the confining stress–axial stress are also plotted in the Fig. 2. The irreversible axial inelastic strain in the specimen before the sleeve broke was 0.06, considerably lager than that observed in uniaxial compression (~0.01). Due to an imperfection in the MTS displacement recording system, the axial strain obtained using the crosshead displacement may contain some errors, which makes an accurate determination of the initial yield stress difficult. Fortunately, the initial yield stress on the linear elastic stress–strain curve can be determined from the axial stress–hoop strain data based on the fact that the sleeve yielded only after the initial plastic deformation of the Vit 1 specimen. The elastic or the yield limit of Vit 1 at the current confining stress is around 2.11 GPa, which is slightly higher than that reported from the uniaxial compression experiments, namely, 1.9 GPa. The specimen failed by abrupt shear band propagation immediately after the confining sleeve failed in the hoop direction. Such a catastrophic shear failure was not expected to occur had the surrounding sleeve remained intact.

The maximum confining stress increased to 761 MPa when the b/a ratio was increased to 1.4. Inelastic deformation of more than 0.09 was attained for the Vit 1 specimen prior to failure of the confining sleeve in the hoop direction. The same conclusion as before can be made that the sleeve yielded at a confining stress of 573 MPa, which is substantially larger than the confining stress at the elastic limit of Vit 1 specimen. The axial stress corresponding to the elastic limit in this case is 2.23 GPa.

As the ratio b/a increased to about 2.0, the confining sleeve began to yield after the confining stress was larger than about 805 MPa, which is once again larger than the confining stress at the elastic limit of the Vit 1 specimen. In contrast to the experiments at smaller b/a ratios, maximum axial stress of 3.81 to 4.15 GPa was achieved and was limited by the strength of the tungsten carbide inserts instead of by the plasticity/failure of the confining sleeve. The permanent inelastic deformation of Vit 1 that was measured can be as high as 0.1. It is interesting to note that some macroscopic shear slips occurred on the Vit 1 specimens, which might be due to material imperfection that nucleated the slip steps. However, such shear slip propagation was further restricted and stabilized by the confining stress imposed by the sleeve.

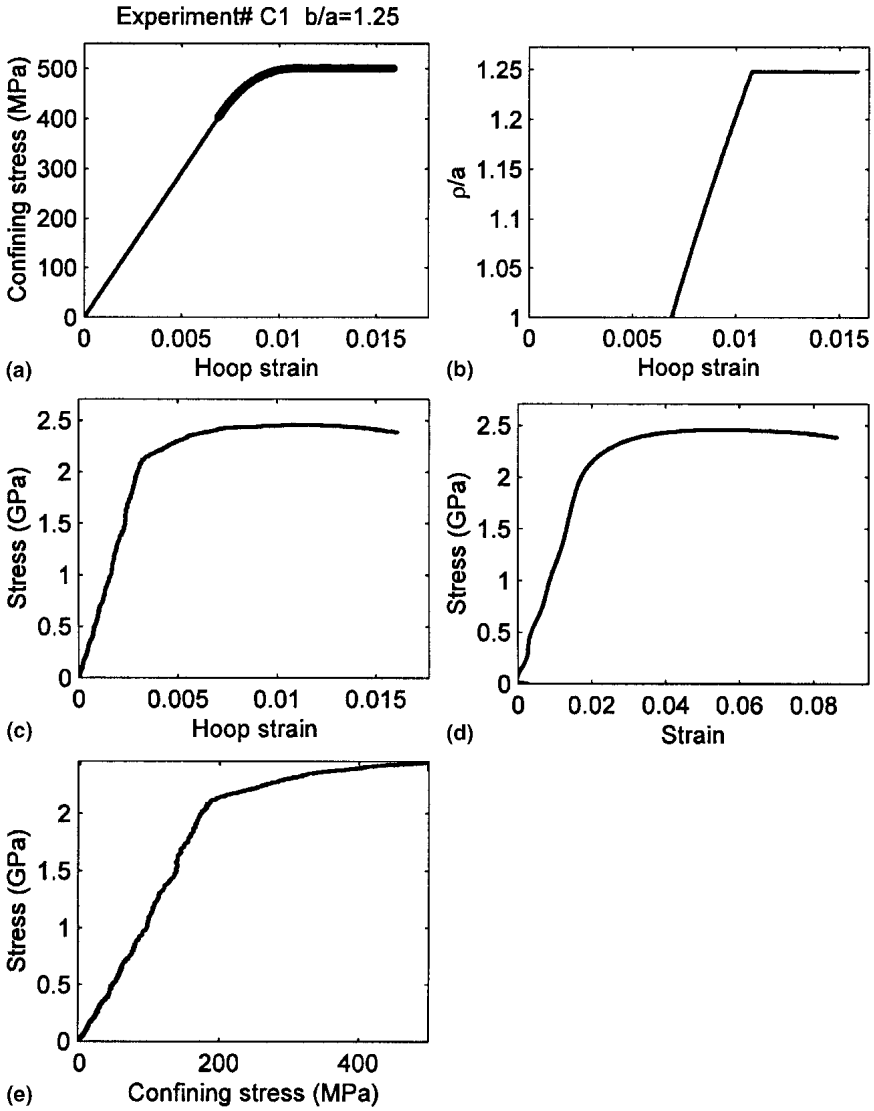

FIG. 2. Multiaxial compression of Vitreloy 1 using a confining sleeve with $b/a = 1.25$: (a) plot of model description of confining stress versus hoop strain, (b) plot of model description of plastic/elastic interface versus hoop strain, (c) plot of experimental axial stress versus hoop strain, (d) plot of experimental axial stress versus axial strain, and (e) plot of axial stress as a function of confining stress based on the experiment and the model.

Confining stress as high as 1.7–1.88 GPa was reached for thicker confinement sleeves, as *b/a* was increased to a value of 5. Further increase in the *b/a* ratio results in insignificant increase in the confining stress. The sleeves did not fully yield for these thicker geometries, and the maximum lateral stress of 1.05 GPa was achieved before the inner surfaces of the sleeves began to deform plastically. The permanent inelastic strain achieved in the specimens in these cases was in the range of 0.03–0.06 before the tungsten carbide inserts failed. Post-examination of recovered specimens reveal that a significant level of overall inelastic deformation observed in metallic glass under confinement is due to (i) considerable amount of multiple shear band formation and (ii) the effect of multiaxial state of stress in stabilizing the otherwise catastrophic propagation of shear bands. The observed large inelastic deformation under confined conditions is consistent with earlier observations.[19]

One critical factor in the measurement of the confining stress is the closeness of fit between the confining sleeves and the specimens. The measurements were based on the assumption that the sizes of the specimens were perfectly matched with their sleeves; that is, there is no overlap or gap before the specimens were inserted to the sleeves. However, it is impossible to achieve such perfection, and to some degree, albeit small, dimensional mismatch is present. To reduce the uncertainty due to this dimensional mismatch, both the sleeves and the specimens were specially ground and honed such that the diameter of the specimen is equal or larger than inner diameter of

the sleeves. Hence, the mismatch in the diameters is within 5 μm, which in turn results in a lateral prestress of around 0–75 MPa, estimated based on the linear elastic theory and the mechanical properties of both Vit 1 and C300 steel. Consequently, this confining stress is quite small compared to the confining stress of 450–1880 MPa at the onset of yield in Vit 1. The effect of the friction between the sleeve and the specimen was minimized by applying high-pressure lubricant, but the determination of the influence due to this friction is not straightforward. Although there exist these limitations in the current experimental technique, the method of confining sleeve is still useful as a first step in exploring and understanding the inelastic deformation behavior of metallic glasses subjected to high confining stresses.

The confining apparatus used in this investigation is probably the simplest one that can provide a lateral stress of as high as 2 GPa. Pressure vessels filled with pressurized liquid/gas usually provide pressures in the range of up to 700 MPa.[19] However, a drawback of the current technique is that it cannot provide a constant confining stress on the specimen, and, furthermore, the lateral stress is dependent on the frictional interaction between the specimen and the sleeve. Nevertheless, the above experimental results have demonstrated the feasibility of the experimental setup in achieving very high confining stresses.

B. Shear bands

All the confining sleeves with b/a ratio less than 1.4 broke in their hoop direction, and the specimens confined by those sleeves were sheared off. For other experiments in which the sleeves remained undamaged, the specimens were recovered by carefully pressing them away from their confining sleeves. The axial stress applied to the specimens to remove them was not sufficient to create further inelastic deformation. The shear slips on the lateral surfaces due to the shear banding of the deformed specimens were then examined using scanning electron microscopy (SEM). Figure 3(a) illustrates a low magnification view of shear slip on the lateral surface of a specimen (C1) confined by a sleeve with $b/a = 1.25$. The fracture surface seen at the upper right-hand corner of the figure was formed after the confining sleeve failed. In contrast to crystalline materials, particularly metals, whose plastic deformation is attributed to mobility of dislocations, the macroscopic inelastic deformation of metallic glasses takes place at much larger scales, highly localized within narrow shear bands. The shear bands shown in Fig. 3(a) are distributed in a uniform manner and their typical width is about 1–2 μm. The direction of a typical shear slip, determined based on the grinding marks on the surface of the specimen, whose direction is perpendicular to the loading axis, forms an angle of 45° with respect to the loading axis. A large shear induced local sliding is manifested in Fig. 3(b) in which a 20-μm relative shear offset is observed, which could have occurred after the sleeve was broken. The surface morphology of the major sheared surface following the damage of the confining sleeve is shown in Fig. 3(c), where the presence of a "vein" pattern indicates that the local temperature may have increased substantially during shear failure.

Further increase in the confining stress produced very similar shear slip patterns, as depicted in Figs. 3(d) and 3(e). It is important to note that all the slip lines are oriented at 45° with respect to the loading axis as evidenced by the grinding marks on the surfaces of the specimens. It is worth mentioning that shear bands were created not only in one direction, but also in multiple directions [Fig. 3(e)], forming families of conjugate slip, which might depend on the geometrical (surface) imperfections or the statistical distribution of the material properties, including the free volume.

IV. FLOW CRITERION

It has been well established that excess free volume plays an important role on the flow behavior of amorphous materials such as metallic glasses.[25–28] As mentioned in Sec. I, there exists experimental evidence supporting the hypothesis that free volume is a function of the inelastic deformation of metallic glasses. Early results[12,15] suggested that metallic glasses obey von Mises flow criterion. However, it appears that no physical mechanism at the microscopic level supports such a flow criterion that is independent of pressure. Davis and Kavesh[13] were probably the first to report the pressure dependency of flow stress in metallic glass by using a liquid pressure system that can generate the confining stresses of up to 620 MPa. The pressure dependence of flow stress was found to be $\Delta\sigma/\Delta P \cong 0.077$ for stress states in compression and the ratio between the yield stress in uniaxial compression to that in uniaxial tension was found to be $\sigma_c/\sigma_t \cong 1.053$.

All principal stresses, including the intermediate stress, play important roles in determining the flow stress of polycrystalline materials due to the limited number of slip planes and the interactions of individual grains and irregular grain boundaries. On the other hand, amorphous metallic glasses have an isotropic structure at the microstructural level, resulting in equal possibility of slipping in any direction, which in turn implies that the intermediate stress may not be critical in affecting the flow stress although it might contribute to the pressure dependent character of the flow. As a consequence, for Vit 1, one might use a normal stress-dependent Mohr–Coulomb criterion, which has been widely used in describing the mechanics of flow in soils and polymers,

$$\tau = \tau_0 + \alpha\sigma_n \quad , \tag{7}$$

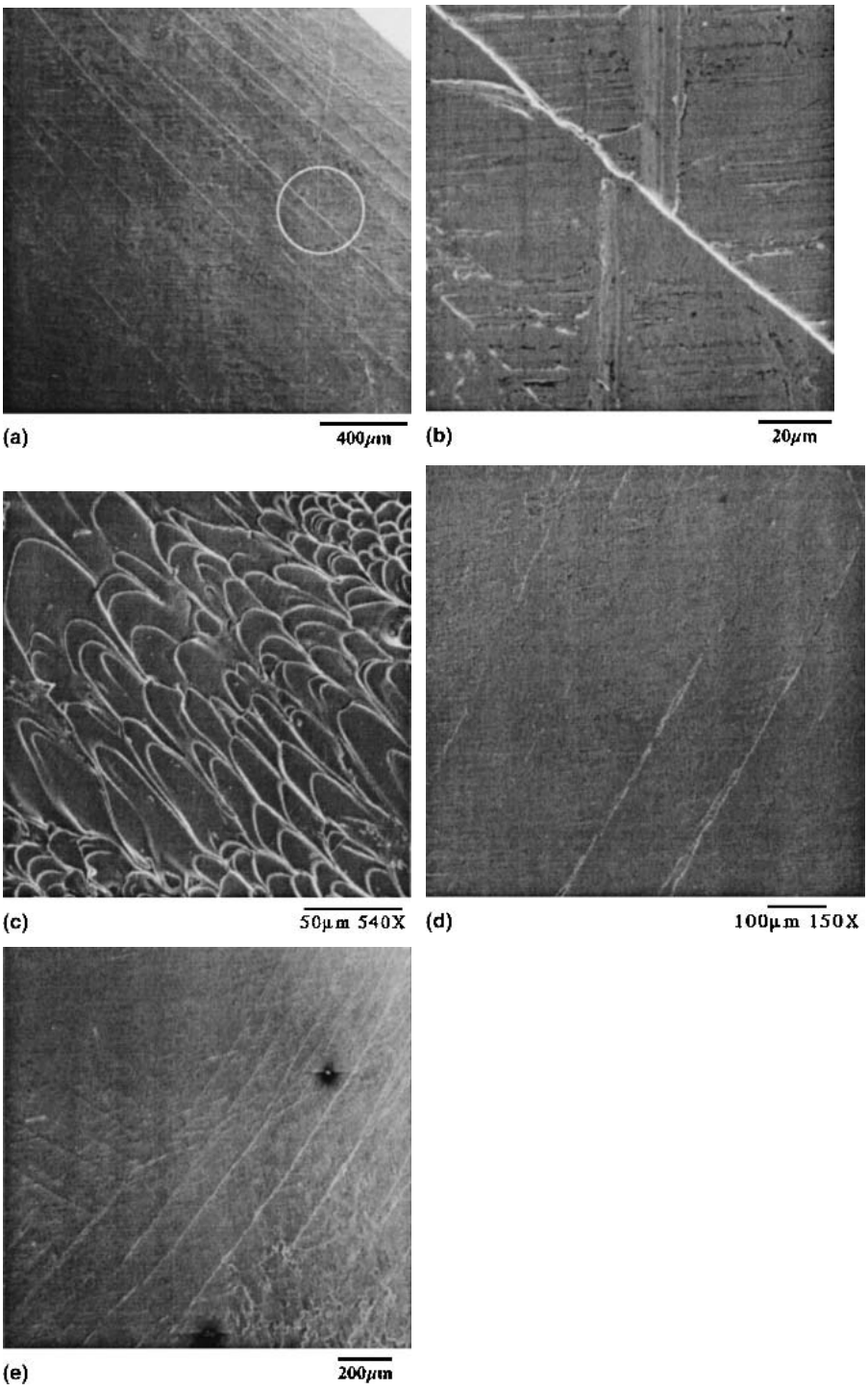

FIG. 3. (a) SEM micrograph of shear bands on the surface of deformed specimen (experiment #C1) confined by a sleeve with ratio $b/a = 1.25$; (b) enlarged view of shear slips on the surface of specimen in Fig. 3(a) (experiment #C1); (c) shear failure surface of specimen (experiment #C1) due to failure of the confining sleeve; (d) SEM micrograph of shear bands on the surface of deformed specimen (experiment #A2) confined by a sleeve with ratio $b/a = 1.4$; (e) shear bands in multiple directions (conjugate) on the surface of a deformed specimen (experiment #A2).

where τ_0 is the cohesive shear stress, τ and σ_n are the shear stress and the normal stress components on the slip plane and in the directional normal to the slip plane, respectively, where the inelastic or plastic flow occurs; and α is a parameter related to the normal stress dependence. The dependence is strongly affected by the parameter α and the criterion will degenerate to Tresca flow criterion if α is zero.

Donovan[14] performed compression, tension, and shear experiments on a Pd–Ni–P metallic glass and concluded that a normal stress dependent Mohr–Coulomb is suitable to describe the yield behavior of the glass and the coefficient of the normal stress dependence α is 0.113. Lewandowski and Lowhaphandu[19] performed a series of tensile experiments on Vit 1 with constant lateral confining stress of up to 700 MPa, which was generated by a pressure vessel. Their experimental results suggest that the influence of hydrostatic pressure on the flow behavior of Vit 1 is relatively small. However, the average angle between the fractured plane and the loading axis in the specimens was found to be 39.4–42.2°, which appears to be more consistent with a normal stress dependent Mohr–Coulomb flow criterion. The coefficient of the normal stress dependence α was in a range of 0.04.[19] More recently, Wright *et al.*[9] suggested from their uniaxial compression experiments that Vit 1 might follow a Mohr–Coulomb flow criterion with a coefficient of normal stress dependence α of 0.105.

Based on the current confinement experiments, one is able to systematically explore the influence of confining stress on flow stress at different stress states; thus the influence of hydrostatic pressure and normal stress on the flow behavior of metallic glasses. It is widely recognized that there is no strain hardening associated with the post-yielding of metallic glasses. For the typical six experiments performed and listed in Table II, three or four stress states were selected from each experiment: one near the initial yielding state, another corresponds to a state near the maximum confining stress, and the other stress state(s) was (were) somewhere in between the two states. The principle stresses in the present experiments are (σ_c, σ_c, σ) where σ is the axial stress and σ_c is the radial confining stress. For instance, four stress states (in the form of (σ_c, σ_c, σ) after the specimen yielded were used from experiment #B4. They are (434, 434, 2480), (602, 602, 2740), (1000, 1000, 3320), and (1508, 1508, 4050) (units: MPa). In addition, two stress states associated with two uniaxial compression experiments were also included. A total of 23 representative stress states were utilized. The Mohr circle associated with each stress state can be easily determined; the center of each Mohr circle is the average value of the confining stress and the axial stress, whereas the radius of the circle is half of the difference between the axial stress and the confining stress. The Mohr circles corresponding to the stress states of the yielded Vit 1 specimens are plotted in Fig. 4. The normal stress and the associated shear stress at any point of each Mohr circle can be easily determined graphically.

The average slope of the envelope of the Mohr circles (Fig. 4) from the current experimental results reveals that $\alpha = 0.16$ [Eq. (7)]. If the Mohr–Coulomb criterion is appropriate for Vit 1, then the angle of the critical shear plane with respect to the lading axis should be around 40°. However, the SEM examination of shear bands in deformed specimens as depicted in Fig. 5 clearly indicate that all the slip (shear) planes were formed at an angle of 45 ± 1° to the loading axis, if one refers to the grinding marks on the surfaces of the specimens which are initially perpendicular to the loading axis. This inconsistency

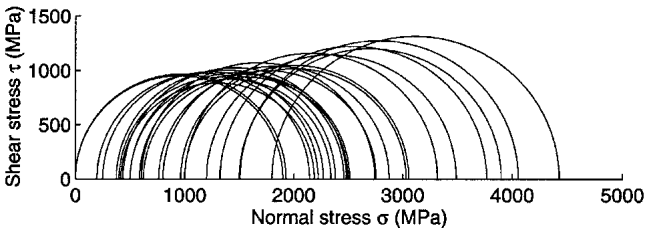

FIG. 4. Mohr–Coulomb circles for Vitreloy 1 deduced from the experimental data.

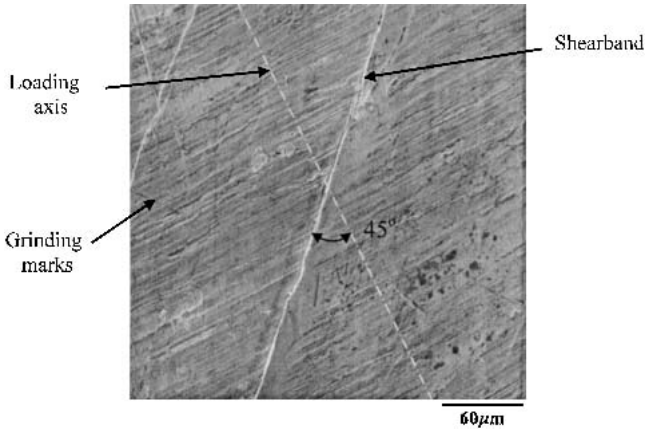

FIG. 5. SEM micrograph of shear bands on the surface of deformed specimen (experiment #C4) confined by a sleeve with ratio $b/a = 4.0$. Note the shear band is oriented at 45° to the compressive loading axis.

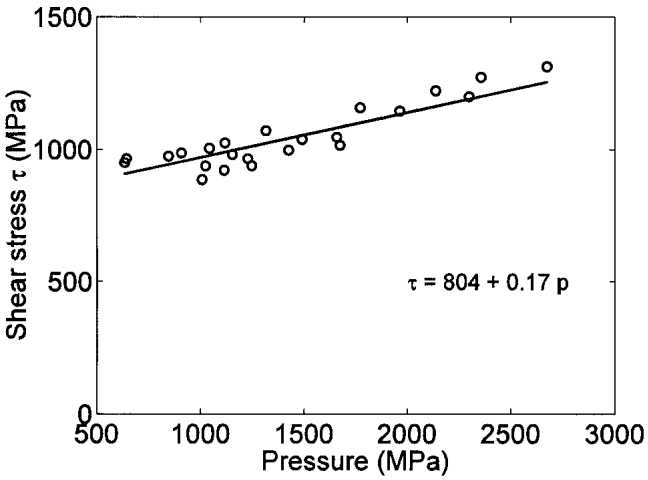

FIG. 6. Plot of the maximum shear stress as a function of hydrostatic pressure for Vitreloy 1.

suggests that a normal stress dependent flow criterion may not be appropriate to describe the flow behavior of Vit 1. In the normal stress dependent Mohr–Coulomb model [Eq. (7)], the intermediate principal stress exerts no influence on the yield behavior. Instead, one could consider a pressure dependent model by modifying the well-known Tresca criterion,

$$\tau = \tau_0 + \beta p \quad , \tag{8}$$

where $p = \sigma_{ii}/3$ is the hydrostatic pressure (σ_{ii} is trace of the stress tensor, σ), and β is the pressure dependency parameter. This model indicates that the critical shear stress is a function of the maximum and minimum principle stress, as well as the hydrostatic pressure. The influence of the intermediate stress is through the effect of the hydrostatic pressure. This model also implies that the maximum shear direction is always 45° to the axis of the loading direction in multiaxial compression experiments with uniform lateral confinement, and the critical shear stress is dependent on the hydrostatic pressure. The experimentally obtained value of β is 0.17 for the metallic glass Vit 1, i.e., the slope of the maximum shear stress versus the hydrostatic pressure shown in Fig. 6.

V. CONCLUSIONS

The following conclusions can be drawn regarding the role of confinement on the mechanical behavior of metallic glasses based on the investigation of the bulk metallic glass Vitreloy 1 subjected to multiaxial compression.

(1) The metallic glass Vitreloy 1 exhibits a considerable amount of inelastic strain, more than 10%, if subjected to axial compression accompanied by lateral confinement. This is in contrast to its "brittle" behavior (shear failure) under uniaxial compression loading conditions. The large inelastic deformation under confinement is realized through the accumulation of multiple shear bands at a microstructural scale larger than dislocations in polycrystalline metals.

(2) Detailed examination of the orientation of the shear slip on the surfaces of the recovered specimens, 45° to the loading axis, suggests that the critical shear stress for flow in metallic glass is not necessarily a function of the normal stress but rather controlled by the hydrostatic pressure. This implies that a pressure dependent flow model is more appropriate than a normal stress-dependent Mohr–Coulomb criterion for bulk metallic glasses, in particular for Vit 1. This observation appears to be in contrast to those of previous results[12,14–19] regarding the flow criterion of metallic glasses.

It is clear that large inelastic deformation in metallic glasses can be achieved using a mechanism (either external loading or microstructural) to arrest catastrophic shear failure and by promoting multiple shear band formation. Creating multiaxial loading condition using confining sleeves as has been demonstrated in this study can effectively enhance the macroscopic inelastic flow of Vit 1. Another way of arresting and retarding shear band propagation of monolithic Vit 1 is the introduction of a second ductile phase as reinforcement, and such a composite has been realized by Hays *et al.*[29] by adding a small amount Nb and slightly altering the original Vit 1 composition. The mechanism associated with shear band arrest in such a composite appears to be different from that attained using the confining sleeve and deserves further attention.

ACKNOWLEDGMENTS

This work was sponsored by the Structural Amorphous Metals Program of the Defense Advanced Research Projects Agency (DARPA), under ARO Contract No. DAAD19-01-1-0525, and in part by the Center for Science and Engineering of Materials at the California Institute of Technology through a grant from the MRSEC program of the National Science Foundation, which are gratefully acknowledged. The authors thank Professor W.L. Johnson for providing the facilities for processing of the material used in the study and for many helpful discussions.

REFERENCES

1. W.J. Klement, R.H. Willens, and P. Duwez, Nature **187,** 869 (1960).
2. H.S. Chen and D. Turnbull, Acta Metall. **17,** 1021 (1969).
3. C.A. Pampillo, J. Mater. Sci. **10,** 1194 (1975).
4. T. Masumoto and R. Maddin, Mater. Sci. Eng. **19,** 1 (1975).
5. A. Inoue, *Bulk Amorphous Alloys: Preparation and Fundamental Characteristics* (Trans Tech Publications, Uetikon-Zuerich, Switzerland, 1998).
6. W.L. Johnson, MRS Bull. **24,** 42 (1999).
7. A. Peker and W.L. Johnson, Appl. Phys. Lett. **63,** 2342 (1993).
8. C.J. Gilbert, V. Schroeder, and R.O. Ritchie, Metall. Mater. Trans. A, **30A,** 1739 (1999).
9. W.J. Wright, R. Saha, and W.D. Nix, Mater. Trans. JIM **42,** 642 (2001).
10. W.L. Johnson, JOM **54,** 40 (2002).
11. J. Lu, G. Ravichandran, and W.L. Johnson, Acta. Mater. (in press, 2003).
12. H.A. Bruck, T. Christman, A.J. Rosakis, and W.L. Johnson, Scripta Metall. **30,** 429 (1994).
13. L.A. Davis and S. Kavesh, J. Mater. Sci. **10,** 453 (1975).
14. P.E. Donovan, Acta Metall. **37,** 445 (1989).
15. H. Kimura and T. Masumoto, Acta. Metall. **28,** 1663 (1980).
16. R. Vaidyanathan, M. Dao, G. Ravichandran, and S. Suresh, Acta Mater. **49,** 3781 (2001).
17. P. Lowhaphandu and J.J. Lewandowski, Scripta Metall Mater. **38,** 1811 (1998).
18. P. Lowhaphandu, S.L. Montgomery, and J.J. Lewandowski, Scripta Metall. **41,** 19 (1999).
19. J.J. Lewandowski and P. Lowhaphandu, Philos. Mag A. **82,** 3247 (2002).

20. J. Lu, PhD Thesis, California Institute of Technology, Pasadena, CA (2002).
21. Y.J. Kim, R. Busch, W.L. Johnson, A.J. Rulison, and W.K. Rhim, Appl. Phys. Lett. **65,** 2136 (1994).
22. A. Masuhr, T.A. Waniuk, R. Busch, and W.L. Johnson, Phys. Rev. Lett. **82,** 2290 (1999).
23. K. Oguni, C.Y. Tan, and G. Ravichandran, J. Compos. Mater. **34,** 2081 (2000).
24. Z. Ma and K. Ravi-Chandar, Exp. Mech. **40,** 38 (2000).
25. A.S. Argon, Acta Metall. **27,** 47 (1979).
26. F. Spaepen, Acta Metall. **25,** 407 (1977).
27. P. de Hey, J. Sietsma, and A. Van den Beukel, Acta Metall. **46,** 5873 (1998).
28. K.M. Flores, D. Suh, R. Howell, P. Asoka-Kumar, P.A. Sterne, and R.H. Dauskardt, Mater. Trans. JIM **42,** 619(2001).
29. C.C. Hays, C.P. Kim, and W.L. Johnson, Phys. Rev. Lett. **84,** 2901 (2000).